METEOROLOGY AND STRATEGIES FOR USING PLANT ATTRACTANTS IN ADULT NOCTUID SUPRESSION PROGRAMS

John K. Westbrook and Peter D. Lingren

USDA-ARS, Areawide Pest Management Research Unit
2771 F&B Road, College Station, TX 77845

ABSTRACT

Atmospheric variables can strongly impact the efficacy of plant-derived attractants used as lures for suppression of noctuid pest insects. Relevant meteorological measurements are discussed that describe release rates of volatile plant compounds, effects of the local atmospheric environment on the spatial distribution of the volatile compounds, and the range of olfactory response of target pest insects to volatile plant compounds. Gaussian plume dispersion simulations using a 2-m source height estimated maximum volatile concentrations 500 m down at the surface that were 36 times greater for moderately stable atmospheric conditions than for extremely unstable conditions. The simulations also revealed that the maximum volatile concentration was located 50 m farther downwind for moderately stable atmospheric conditions than for extremely unstable atmospheric conditions. Potential for development of adult control and monitoring technology will be enhanced by understanding and properly monitoring spatial and temporal characteristics of atmospheric properties within the pest biosphere.

INTRODUCTION

Adult noctuids have been found to feed, mate, and oviposit in numerous species of native plants and cultivated crops (Lingren et al. 1989). Volatile chemical compounds (i.e., plant attractants) or bouquets from these attractive plants have been shown to attract adult noctuids (Lingren et al. 1989; Tingle and Mitchell 1992). Hierarchical host preference structures have been identified for *Heliothis* species (Fitt 1989). The polyphagous nature, mobility and fecundity of several noctuid species suggest that the pest should be controlled in their more susceptible adult stage before the subsequent generation of larvae has infested vast host crop areas (Knipling 1979).

Studies of adult noctuid behavior have shown distinct temporal patterns of emergence, flying, feeding, mating, and ovipositing. Lingren et al. (1988) pointed out that knowledge of the temporal patterns of adult insect behavior could be used to target the use of adult feeding attractant control technologies, but cautioned that well-fed, previously-mated immigrant females may oviposit before feeding.

The potential use of plant attractants has been a major component of adult control technologies (Lingren et al. 1989). Plant attractants, unlike sex pheromones, are able to attract males and females. Plant attractants can be contaminated with insecticide or placed inside traps near host habitats to attract and kill adult noctuids (Lingren et al. 1989, 1990).

Any control strategy using plant attractants must incorporate knowledge of the release rate of volatile compounds and their diffusion above and within host plant canopies. Ambient

atmospheric features are identified that will lead to strategic use of plant attractants for control of adult noctuids. The dispersion of plant attractants is simulated here using only mean atmospheric profiles, but higher-resolution atmospheric processes are discussed. Higher-resolution measurements of atmospheric processes require intensive and costly field data to define microscale atmospheric turbulent processes.

METHODS

Release Rate of Plant Attractants. Plant attractants must be released at appropriate rates to be effective in strategies for controlling adult noctuids. Further, maintaining biologically-effective release rates will yield more efficient use of the volatile compounds, less cost, and less frequent administration of the material. Baker (1987) described two indices that are valuable to the comparison of various plant attractant formulations: the Therapeutic Index *(TI)* and Dosage form Index *(DI)*. The Therapeutic Index is defined as:

$$TI = \frac{minimum\ toxic\ concentration}{minimum\ effective\ concentration} \quad (1)$$

where a greater value of *TI* implies a wider window of acceptable release rates. The Dosage form Index is expressed as:

$$DI = \frac{maximum\ concentration\ \text{in}\ dosage\ cycle}{minimum\ concentration\ \text{in}\ dosage\ cycle} \quad (2)$$

where a lesser value of DI implies a more constant release rate, ideally maintaining a concentration of volatiles in the effective range for insect control. The diffusion of volatile compounds from various substrates may be categorized as sustained-release and controlled-release systems. Sustained-release systems are strongly influenced by their environment. Alternatively, controlled-release systems, which will be discussed exclusively hereafter, maintain release rates that are largely independent of environmental factors. Five primary controlled-release formulation types are: microcapsules, trilaminates, capillaries, ropes, and liquid flowables (Weatherston 1990). The stability and longevity of formulations can be adversely affected by ultraviolet light, pH, metal ions, adsorption, and desorption (Weatherston 1990).

Continuous release rates of volatile compounds are generally categorized by one of three differential equations (Baker 1987). Zero-order, first-order, and square-root-of-time release rates are represented by the three respective equations that follow:

$$\frac{dM_t}{dt} = \beta \quad (3)$$

$$\frac{dM_t}{dt} = \beta\, M_0 \exp(-\beta\, t), \text{ and} \quad (4)$$

$$\frac{dM_t}{dt} = \frac{\beta}{\sqrt{t}} \quad (5)$$

where M_t is the mass of volatile material at time t, β is the release rate coefficient, and M_0 is the initial mass of volatile material. The time at which M_t equals half the value of M_0 is referred to as the half-life ($t_{½}$) of the volatile material. The time at which M_t equals the minimum value that is detectable by the target organism is referred to as the effective time (t_e) of the volatile material. Leonhardt et al. (1990) found that the release rate of grandlure from laminate dispensers increased substantially with increasing temperature in the range of 30 to 60°C. Brown et al. (1992) found a considerable change in the blend of volatile compounds released from a polyethylene dispenser due to differential release rates of each component.

Dispersion of Plant Attractants. Movement of volatile compounds from a source can be described by three processes: advection by the wind, molecular diffusion, and turbulent mixing. In the boundary layer of the plant canopy, these processes are governed by differential heat exchange and frictional effects. The process of advection is readily modeled by the scalar product of the three-dimensional fields of wind velocity and the concentration of the dispersing material. Molecular diffusion, likewise, is a well-defined process for known values of barometric pressure, air temperature, absolute humidity, and wind speed. Turbulent mixing, however, occurs over a broad spectrum of space and time scales. Current theory and instrumentation can only approximate the impact of turbulent mixing on the spread of airborne materials.

Temperature Lapse Rate. Net radiation, differential heat capacity, and differential heat conductance cause the vertical profile of air temperature (lapse rate) to vary diurnally. Further, the lapse rate may vary considerably with altitude and location. Lapse rates are broadly categorized as stable, neutral, and unstable. A neutral lapse rate (9.8°C/km) indicates that an air parcel which is forced to ascend or descend adiabatically (i.e., without exchanging heat with the ambient atmosphere) will remain neutrally buoyant. A stable lapse rate (< 9.8°C/km) will force an ascending or descending air parcel to return to its initial height. Conversely, an unstable lapse rate (> 9.8°C/km) will cause an air parcel to continue moving vertically. Thermal convection (due to atmospheric buoyancy differences) is enhanced when the lapse rate becomes unstable. Unstable lapse rates are generally created when a surface such as dry soil is heated, more than the ambient air, by insolation. By its very nature, an unstable lapse rate is a transient phenomenon. Conversely, a stable lapse rate can persist for hours or days. Fig. 1 shows the relationship between lapse rates and atmospheric mixing. Note that a discontinuity in the vertical stability exists for cases of fumigation and lofting.

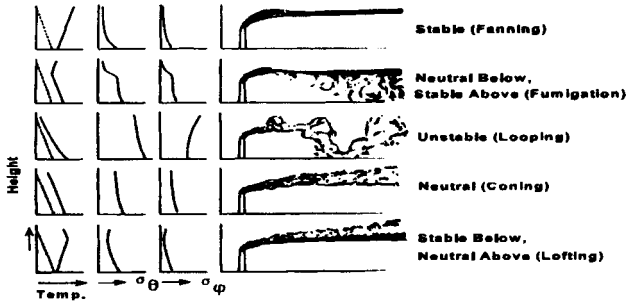

FIG. 1. Various types of smoke plume patterns observed in the atmosphere. The dashed curves in the left-hand column of diagrams show the adiabatic lapse rate, and the solid lines are the observed temperature profiles. The abscissas of the columns for the standard deviation of the horizontal and vertical wind direction (σ_θ and σ_φ, respectively) represent a range of about 0° to 25° (after Slade 1968).

Water Vapor. Air density decreases with increasing atmospheric vapor content. Because atmospheric water vapor content contributes to atmospheric buoyancy, it is often incorporated with temperature in a parameter called virtual temperature (T_v). Soil heat capacity and conductance changes markedly with increased soil moisture due to latent heat of (water) vaporization. Therefore, dry soil and ambient air will be heated much more than moist soil and ambient air because more incident solar radiation will be partitioned to sensible heat than to latent heat of vaporization.

Wind Shear. The vertical gradient of wind velocity – a vector quantity possessing speed and direction – is known as wind shear. Wind shear can be expressed as the vertical gradient of wind speed and/or the vertical gradient of wind direction. In this paper, we will refer exclusively to the vertical gradient of wind speed as wind shear. The vertical profile of wind speed in the neutrally-stable atmospheric boundary layer follows a logarithmic relationship (Spillman 1984):

$$\bar{u} = \frac{u_*}{k} \ln\left(\frac{z - d}{z}\right) \tag{6}$$

where $\bar{u}$ is the mean wind speed at height z, k is the von Karman constant (0.40), u_* is the friction velocity, d is the zero-plane displacement, and z_0 is the surface roughness. Friction velocity is equal to the square root of the vertical flux of horizontal momentum near the surface divided by the average ambient air density. Zero-plane displacement is the distance above the ground at which the wind speed, extrapolated downward from well above the ground cover, is estimated to be zero. Representative values of surface roughness are listed in Table 1. For non-neutral stability, the wind profile equation (Equ. 6) is changed to (Spillman 1984):

$$\bar{u} = \frac{u_*}{k} \left[\ln\left(\frac{z - d}{z}\right) + \beta' \left(\frac{z}{L'}\right)\right] \tag{7}$$

where $\beta' \approx 7$ for stable conditions and $\beta' \approx 4.5$ for unstable conditions. L' is the Monin-Obukhov length which can be determined from measurements of the vertical gradients of air temperature and wind speed and is expressed as:

$$L' = \frac{u_*}{kg} \frac{(d\bar{u}/dz)\ T}{(dT/dz + \Gamma)} \tag{8}$$

where T is air temperature (°K) and Γ is the adiabatic lapse rate of temperature (9.8°K/km). Bache and Unsworth (1977) found that a cotton canopy in a stable atmospheric boundary layer dissipated a substantial amount of momentum, resulting in a weak wind flow beneath the canopy that was decoupled from the wind above the canopy. Decoupled air flow within a cotton canopy was also noted in the release of a volatile compound (the sex pheromone, gossyplure) for control of the pink bollworm, *Pectinophora gossypiella* (Saunders) (Flint et al. 1993).

Wind shear leads to mechanical convection which can erode unstable lapse rates. However, thermal convection tends to erode wind shear. The buoyant force and shear force are often expressed in a parameter known as the Richardson number (Kaimal and Finnigan 1994):

$$Ri = \frac{g}{\bar{\theta}} \frac{\partial\theta/\partial z}{(\partial\bar{u}/\partial z)^2} \quad (9)$$

where g is gravitational acceleration, and θ is mean potential temperature (°K). Positive values of the Richardson number indicate stable atmospheric conditions, and vice versa. Air flow begins to change from turbulent to laminar at a critical Richardson number of 0.25.

TABLE 1. Typical Values of Surface Roughness (z_0) for Diverse Terrain (After Spillman 1984).

z_0 (m)	Description of Terrain
0.00001	Mud flats, tundra
0.001	Lawn grass
0.007	Downland
0.03	Thick grass, arable crops
0.02 — 0.1	Farmland with hedges, etc.
0.1 — 0.3	Farmland, savannah (i.e., with considerable tree coverage)
0.3 — 1.0	Forests

Turbulence. Atmospheric turbulence results from the dissipation of energy from eddy motions of all spatial and temporal scales. Turbulent mixing, however, is a difficult process to measure or derive from standard meteorological measurements. Turbulent eddies are especially difficult to measure in the surface layer because of varying surface roughness, temperature lapse rates, and the transience of the eddies.

Early estimates of atmospheric dispersion from a steady-state (zero-order release) point source were based on the Gaussian distribution. For example, Pasquill expressed the Gaussian distribution of the steady-state plume with reflection (no adsorption or impaction) at the ground surface in the form (Slade 1968):

$$\bar{\chi} = \frac{Q'}{2\sigma_y\sigma_z\bar{u}} \exp\left(-\frac{y^2}{2\sigma_y^2}\right) \left\{\exp\left[-\frac{(z-h)^2}{2\sigma_z^2}\right] + \exp\left[-\frac{(z+h)^2}{2\sigma_z^2}\right]\right\} \quad (10)$$

where $\bar{\chi}$ is the average concentration, Q' is the release rate, $\bar{u}$ is the mean wind speed, σ is the plume dispersion coefficient, h is the height of release, y is the horizontal crosswind direction, and z is the vertical direction. Equ. 10 requires values of the mean wind speed and standard deviations of the plume dispersion width as a function of distance along the horizontal and vertical coordinate axes. Pasquill turbulence types estimate the degree of atmospheric stability or instability based on the surface wind speed and daytime insolation or nighttime cloud cover, as appropriate (Table 2). Standard deviations of plume dispersion are empirically related to distance for each of the Pasquill turbulence types (Figs. 2 and 3). Various forms of atmospheric diffusion coefficients for Gaussian plume equations are listed in Table 3. Further, the lateral and vertical half-widths of the plume can be expressed (Slade 1968), respectively, as:

$$y_p = \sqrt{2\sigma_y^2 \ln \frac{100}{p}}, \text{ and} \tag{11}$$

$$z_p = \sqrt{2\sigma_z^2 \ln \frac{100}{p}} \tag{12}$$

where p is the required percent (e.g., 50%) of the axial concentration.

TABLE 2. Relation of Pasquill Turbulence Types to Weather Conditions (After Slade 1968).

Surface Wind Speed ($m\ s^{-1}$)	Daytime Insolation[a]			Nighttime Conditions	
	Strong	Moderate	Slight	Thin Overcast or ≥ 4/8 Cloudiness[b]	≤ 3/8 Cloudiness
< 2	A	A - B	B	---	---
2	A - B	B	C	E	F
4	B	B - C	C	D	E
6	C	C - D	D	D	D
> 6	C	D	C	D	D

[a] A - Extremely Unstable, B - Moderately Unstable, C - Slightly Unstable, D - Neutral[c], E - Slightly Stable, F - Moderately Stable.

[b] The degree of cloudiness is defined as that fraction of the sky above the local apparent horizon that is covered by clouds.

[c] Applicable to heavy overcast, day or night.

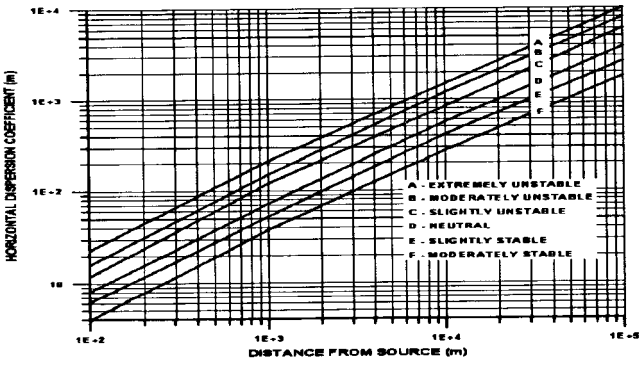

FIG. 2. Lateral diffusion, σ_y, as a function of downwind distance from a point source for Pasquill turbulence types (after Slade 1968).

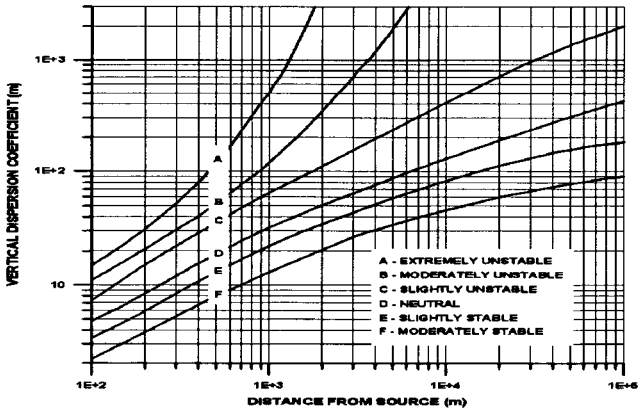

FIG. 3. Vertical diffusion, σ_z, as a function of downwind distance from a point source for Pasquill turbulence types (after Slade 1968).

TABLE 3. Summary of Atmospheric Diffusion Coefficients[a] (After Slade 1968).

Identification	Diffusion Coefficients	Plume Dimensions
Sutton	C_y, C_z, n_y, n_z	$\sigma_y = 2^{-1/2}\, C_y\, x^{(2-n_y)/2}$ $\sigma_z = 2^{-1/2}\, C_z\, x^{(2-n_z)/2}$
Fickian	K_x, K_y, K_z	$\sigma_y = (2\, K_y\, t)^{1/2}$ $\sigma_z = (2\, K_z\, t)^{1/2}$
Cramer	σ_θ, σ_φ, p, q	$\sigma_y = \sigma_\theta\, x^p$ $\sigma_z = \sigma_\varphi\, x^q$
Pasquill	$\sigma_{\theta(T,t)}$, $\sigma_{\varphi(T,t)}$	$\sigma_y = \sigma_{\theta(T,t)}\, x$ $\sigma_z = \sigma_{\varphi(T,t)}\, x$

[a] The symbols T and t represent the sampling time and averaging time, respectively.

The Gaussian form of the plume equation was exclusively in air quality studies until the conception of gradient transfer (K-) theory (Kaimal and Finnigan 1994). K-theory relates turbulent atmospheric diffusivity to wind shear and lapse rate. Vertical profiles of atmospheric diffusivity can be constructed from which to model the vertical component of turbulent dispersion. K-theory defines turbulent flux as down-gradient transport of the associated mean variable (Stull 1988). K-theory works well for small eddies in a neutral

atmospheric boundary layer, but should not be applied to convective mixed layers because large eddies can cause the eddy diffusivity (K) to be negative, indicating that the flux is counter-gradient. Empirical relationships between atmospheric diffusivity and atmospheric stability categories have been summarized (Venkatram and Wyngaard 1988).

Eddy correlation techniques (Haugen 1973) have generally replaced previous methods for estimating turbulent fluxes, but require fast-response (>10-20 Hz) measurements at several locations within a small area. The relationship between eddy correlation values and standard meteorological measurements can be made only by assuming stationarity and homogeneity. However, motions in the atmospheric boundary layer are often nonstationary and nonhomogeneous. Eddy correlation values have been measured for research studies of particular surfaces and atmospheric conditions. Eddy correlation values can reveal high-frequency changes in turbulent phenomena such as vertical fluxes of momentum, heat, and moisture. High-frequency sampling of wind and airborne materials have revealed turbulent bursts. Murlis and Jones (1981) sampled atmospheric ions 15 m downwind of a point source and determined that the ions arrived in discrete bursts that were about 0.1 seconds long and 0.5 seconds apart. Cooper et al. (1992, 1994) used a scanning Raman lidar to measure the spatial and temporal characteristics of the nonhomogeneous turbulent transfer of water vapor over an irrigated orchard and alfalfa pasture. Cooper et al. (1994) found that ramp structures (eddies) were 20 to 30 m in size and had transit lifetimes of 20 to 30 seconds. The lidar provides simultaneous measurements over a large area, unlike conventional point sensors. ReVelle (1993) predicted turbulent bursts accompanied by rapid heating or cooling near the surface that occurred aperiodically as a function of wind speed, wind direction, surface roughness and thermal properties of the soil.

Popular plume modeling techniques now combine a Gaussian distribution laterally and vertically across a meandering plume centerline (Teske et al. 1993), or with random-walk estimates of trajectories of multiple particles. Unlike the standard Gaussian plume model which estimates peak concentrations along the plume centerline, the meandering plume model estimates bimodal peak concentrations along the plume (Murlis et al. 1992).

SIMULATIONS

Dispersion of volatile compounds was simulated using the Pasquill form of the Gaussian dispersion equation (Equ. 10). The simulations assumed a single, steady-state (zero-order release) point source of 1.16×10^{-9} kg/sec at 2 m Above Ground Level (AGL). Simulations were executed for a mean wind speed of 4 m/s at the Pasquill turbulence type D, and at 2 m/s for the other five turbulence types. Estimated concentrations are indirectly proportional to wind speed (e.g., a 5 m/s mean wind speed reduces estimated concentrations to 20% of the respective values at a mean wind speed of 1 m/s).

Maximum downwind concentrations of 1.14×10^{-10} and 1.09×10^{-10} kg/m^3 were located at the surface (0 m AGL) for the A and C turbulence types, respectively. Maximum downwind concentrations for B, D, E, and F, turbulence types were located at 2 m AGL, with values of 1.99×10^{-10}, 7.93×10^{-10}, 1.72×10^{-9}, and 3.44×10^{-9} kg/m^3, respectively. Maximum concentration values were found 10 m downwind for turbulence types A and B, at 20 m for turbulence type C and D, at 40 m for turbulence type E, and at 60 m for turbulence type F. The half-width and half-depth pairs of the estimated Gaussian plumes at 50 m downwind ranged from 2.55 m and 1.53 m for turbulence type F, to 14.81 m and 9.70 m for turbulence type A. The plume dimensions revealed a flat elliptical cross-section, although the vertical dimensions of the plume beyond a distance of 500 m was greater than the lateral dimensions for the A and B turbulence types.

The minimum effective concentrations (10^{12} molecules/m^3) for insect response noted

by Metcalf (1987), when multiplied by the molecular weights shown in Table 4, equals $1.46x10^{-16}$ for amyl alcohol, $1.79x10^{-16}$ for benzyl alcohol, $2.72x10^{-16}$ for eugenol, and $1.99x10^{-16}$ kg/m^3 for phenylacetaldehyde. Volatile plant compounds known to be attractive to various insect species, and other chemical compounds of similar volatility are listed in Table 4. Molecular diffusion of the volatile compounds would add 1.5 to 8.5 m to the lateral and vertical spread from the plume centerline after 12 hrs using the diffusion coefficients listed in Table 4. The limit of minimum effective dimensions at 150 m downwind were a bit narrower for turbulence types B and C (95 m wide and 70 m high, and 85 m wide and 50 m high, respectively). The effective plume dimensions at 350 m downwind were 95 m wide and 65 m high for turbulence type D. Effective plume dimensions at 500 m downwind were 100 m wide and 55 m high for turbulence type E and 65 m wide and 45 m high for turbulence type F. The effective plume width and height generally decreased with increasing atmospheric stability.

In order to achieve complete surface coverage of a field by the effective plume at a distance of 100 m, plant attractant (phenylacetaldehyde) lures would need to be placed at intervals of 200 m, 140 m, 120 m, 60 m, 60 m and 40 m for Pasquill turbulence types A-F, respectively. Turbulence type F represents the "worst-case" scenario and requires five times more lures than for turbulence type A. However, flying noctuids that intercept the higher concentration gradients within the turbulence type F plume may enhance their ability to navigate toward the food (lure) source. Lures would need to be placed around the perimeter of a field to account for varying wind directions. Because noctuids respond to instantaneous concentrations rather than to mean concentrations, complete (inundative) coverage of a field by the effective plume may actually decrease the insects' response to discrete food (lure) sources. Even at locations where the mean concentration is less than the effective concentration, insects may respond to the plume when the instantaneous concentration exceeds the effective level, and begin to search upwind along the plume centerline toward the food (lure) source.

CONCLUSIONS

Meteorological methods are readily available for estimating the mean dispersion of volatile plant compounds used for adult noctuid control. However, instrumentation necessary to measure filament-like, meandering plumes from continuous point sources must be very accurate and responsive. Such instrumentation is expensive, generally requires frequent calibration, and should operate simultaneously at several locations within a field. It is critical to take measurements of the atmospheric environment in which the insects are responsive to the volatile compounds, and at downwind locations if drift is of concern. Fast-response meteorological and chemical sensors are needed to conduct bioassays of individual insect response because insects respond to instantaneous concentrations that may greatly exceed mean concentrations (Murlis et al. 1992). Tracers such as sulfur dioxide, sulfur hexafluoride, phosphorus pentafluoride, smoke and atmospheric ions (Murlis and Jones 1981) may be needed in place of the desired volatile plant compounds to obtain sufficiently fast response measurements using available technologies. Micrometeorological measurements will play a key role in accurate evaluations of field bioassays of volatile plant compounds, enhanced efficacy of treatments, optimized cost of treatments, and reduced dispersion of volatile compounds beyond the target area.

TABLE 4. Physical Characteristics of Volatile Plant Chemicals Attractive as Insect Kairomone (Sources: Metcalf 1987; Fisher Chemical Index 81C; and Aldrich Chemical Catalog Handbook 1984-1985).

Insect Species	Kairomone	Molecular Weight (kg)	Boiling Point (C)	Vapor Pressure[a] (Pa)	Diffusion coefficient[b] ($x10^{-7}$ m^2 s^{-1})
Hylobius pales (Herbst), *Popillia Japonica* (Newman), *Papillio polyzenes asterius* Stoll	Anethole	0.148	234	9.33	---
Eulaema bombiformis	Benzyl acetate	0.150	213	1.33	60
Diabrotica vergifera vergifera LeConte, *Papillio polyzenes asterius* Stoll	Estragole	0.148	216	13.33	---
	Amyl Alcohol	0.088	102	---	72
	Benzyl Alcohol	0.108	205	---	71
Cotinus nitida (L.), *Popillia japonica* (Newman)	Caproic acid	0.116	202-203	---	60
Diabrotica barberi S & L, *Hylobius pales* (Herbst), *Popillia japonica* (Newman), *Andrena* spp., *Euglossa* spp., *Eulaema cingulata*	Eugenol	0.164	254	1.33	38
Acalymma vittatum F., *Diabrotica vergifera vergifera* LeConte	Indole	0.117	253	4	---
Dacus dorsalis Hendel	Methyl eugenol	0.178	254	0.40	---
Helicoverpa zea (Boddie) (& nine other species of Noctuidae), *Cisseps fulvicollis*, *Ostrinia nubilalis* (Hübner)	Phenylacetaldehyde	0.120	195	22.66	---
Diabrotica undecimpunctata howardi	Veratrole	0.138	206	10.66	---

[a] At a temperature of 30° C
[b] At a temperature of 25° C

LITERATURE CITED

Bache, D. H., and M. H. Unsworth. 1977. Some aerodynamic features of a cotton canopy. Q. J. R. Meteorol. Soc. London 103: 122-134.

Baker, R. W. 1987. Controlled Release of Biologically Active Agents. New York: John Wiley & Sons.

Brown, D. F., A. L. Knight, J. F. Howell, C. R. Sell, J. L. Krysan, and M. Weiss. 1992. Emission characteristics of a polyethylene pheromone dispenser for mating disruption of codling moth (Lepidoptera: Tortricidae). J. Econ. Entomol. 85 (3): 910-917.

Cooper, D. I., W. E. Eichinger, D. E. Hof, D. Seville-Jones, R. C. Quick, and J. Tiee. 1994. Observations of coherent structures from scanning lidar over an irrigated orchard. Agric. For. Meteorol. 67: 239-252.

Cooper, D. I., W. E. Eichinger, D. B. Holtkamp, R. R. Karl Jr., C. R. Quick, W. Dugas, and L. Hipps. 1992. Spatial variability of water vapor turbulent transfer within the boundary layer. Boundary-Layer Meteorol. 61: 389-405.

Fitt, G. P. 1989. The ecology of *Heliothis* species in relation to agroecosystems. Annu. Rev. Entomol. 34: 17-52.

Flint, H. M., A. K. Yamamoto, N. J. Parks, and K. Nyomura. 1993 Aerial concentrations of gossyplure, the sex pheromone of the pink bollworm (Lepidoptera: Gelechiidae), within and above cotton fields treated with long-lasting dispensers. Environ. Entomol. 22 (1): 43-48.

Haugen, D. A. (ed.). 1973. Workshop on Micrometerology. Am. Meteorol. Soc., Boston, MA.

Kaimal, J. C., and J. J. Finnigan. 1994. Atmospheric Boundary Layer Flows: Their Structure and Measurement. Oxford, England: Oxford University Press.

Knipling, E. F. 1979. The basic principles of insect population suppression and management. USDA-ARS Tech. Rep. 512.

Leonhardt, B. A., R. T. Cunningham, W. A. Dickerson, V. C. Mastro, R. L. Ridgway, and C. P. Schwalbe. 1990. Dispenser design and performance criteria for insect attractants. p. 113-129. *In* Behavior-modifying Chemicals for Insect Management: Applications of Pheromones and Other Attractants., Ridgway, R. L. Silverstein, R. M., and Inscoe, M. N. eds. Marcel Dekker, Inc., New York.

Lingren, P. D., W. B.Warner, Raulston, J. R., M. Kehat, T. J. Henneberry, S. D. Pair, A. Zvirgzdins, and J. M. Gillespie. 1988. Observations on the emergence from natural populations of corn earworm, *Heliothis zea* (Boddie) (Lepidoptera: Noctuidae). Environ. Entomol. 17 (2): 254-258.

Lingren, P. D., Raulston, J. R. Shaver, T. N., and Teranishi, R. 1989. ARS *Heliothis zea* Adult Supression System Initiative. Paper presented to USDA, ARS, National Program Staff, Beltsville, MD.

Lingren, P. D., Raulston, J. R., Shaver, T. N., and Wann, E. V. 1990 Mortality of newly emerged adult corn earworms following treatment with a feeding stimulant bait. p. 128-132. Proc. 9th Annu. Hort. Ind(s). Show, Tulsa, OK, Jan. 5-6, 1990.

Metcalf, R. L. 1987. Plant volatiles as insect attractants. CRC Critical Rev. in Plant Science. 5: 251-301.

Murlis, J., J. S. Elkinton, and R. T. Carde. 1992. Odour plumes and how insects use them. Annu. Rev. Entomol. 37: 505-532.

Murlis, J., and C. D. Jones. 1981. Fine-scale structure of odour plumes in relation to insect orientation to distant pheromone and other attractant sources. Physiol. Entomol. 6: 71-86.

ReVelle, D. O. 1993. Chaos and "bursting" in the planetary boundary layer. J. Appl. Meteorol. 32: 1169-1180.

Slade, D. H. (ed.). 1968. Meteorology and Atomic Energy, 1968. U.S. Atomic Energy Commission.

Spillman, J. 1984. Meteorology. Short Course on the Aerial Application of Pesticides, Vol. 1. Cranfield Inst. Tech., Cranfield, England.

Stull, R. B. 1988. An Introduction to Boundary Layer Meteorology. Kluwer Academic Publishers, Dordrecht, Netherlands.

Teske, M. E., J. F. Bowers, J. E. Rafferty, and J. W. Barry. 1993. FSCBG: an aerial spray dispersion model for predicting the fate of released material behind aircraft. Environ. Toxicol. Chem. 12: 453-464.

Tingle, F. C., and E. R. Mitchell. 1992. Attraction of *Heliothis virescens* (F.) (Lepidoptera: Noctuidae) to volatiles from extracts of cotton flowers. J. Chem. Ecol. 18 (6): 907-914.

Venkatram, A., and Wyngaard, J. C., editors. 1988. Lectures on Air Pollution Modeling. Am. Meteorol. Soc., Boston, MA.

Weatherston, I. 1990. Principles of design of controlled-release formulations. p. 93-112. *In* Ridgway, R. L., Silverstein, R. M., and Inscoe, M. N. (eds.). Behavior-modifying Chemicals for Insect Management: Applications of Pheromones and Other Attractants. Marcel Dekker, Inc., New York.